Available online at www.sciencedirect.com
ScienceDirect
Journal of Experimental Animal Science 43 (2007) 237–254
Journal of Experimental Animal Science
www.elsevier.de/jeas

Characterization of a rat model of right-sided heart failure induced by pulmonary trunk banding

Uffe K. Schou[a], Christian D. Peters[a], Soo Wan Kim[b], Jørgen Frøkiær[c], Søren Nielsen[a,*]

[a]*The Water and Salt Research Center, Department of Anatomy, Building 233/234, University of Aarhus, DK-8000 Aarhus C, Denmark*
[b]*Department of Internal Medicine, Chonnam National University Medical School, Gwangju, Republic of Korea*
[c]*Clinical Institute, University of Aarhus, Brendstrupgaardsvej 100, Aarhus, Denmark*

Abstract

Animal models of disease are essential for cardiovascular research. However, animal models of right-sided heart failure are few and remain poorly characterized. The aim with this study was to establish a rat model of right-sided heart failure (HF) using pulmonary trunk banding (PTB) and subsequently to characterize the systemic and cardiac changes in this model, including protein expression of SERCA2 and α-sarcomeric actin. Rats underwent banding or sham operation. To evaluate the development of HF over time three groups were included in this study. They were killed 2–3, 5–7 or 16–17 weeks after operation, respectively. PTB rats showed marked hypertrophy of the right ventricle (RV). Catheterization of the RV showed a three- to four-fold increase in right ventricular systolic and diastolic pressures as well as increased dP/dT max and dP/dT min. Plasma analyses revealed increased liver enzymes in most PTB groups and post mortem examination revealed congestion of the liver as well as formation of ascites and hydrothorax in many PTB rats. Immunoblotting of the RV revealed no changes in SERCA2 or α-sarcomeric actin. In conclusion, PTB was an effective method to

*Corresponding author. Tel.: +45 89423046; fax: +45 86198664.
E-mail address: sn@ana.au.dk (S. Nielsen).

0939-8600/$ - see front matter
doi:10.1016/j.jeas.2006.10.004

induce right-sided HF. The presence of HF was confirmed by severe signs of backward failure in conjunction with markedly elevated RV pressures and reduced RV ejection fraction (EF).

Keywords: Right-sided heart failure; Hypertrophy; Animal models; Pulmonary hypertension; Echocardiography; Pulmonary trunk banding; Actin; SERCA2

Introduction

The role of the right ventricle (RV) in cardiac function and disease has often been neglected as most attention is given to the function of the left ventricle (LV). However, it is well recognized that there is a relationship between the functioning of the two ventricles. Thus, impairment of the RV may influence LV function (or vice versa) (Clyne et al., 1989; Dittrich et al., 1989; Hill and Singal, 1997; Mizushige et al., 1989; Yu et al., 1996). In a state of right ventricular pressure overload this ventricular interdependence may be ascribed to pathologic septal motion, decreased LV preload or other unknown factors (Dittrich et al., 1989; Mizushige et al., 1989; Yu et al., 1996). RV function is an independent predictor of mortality and the development of heart failure (HF) in patients with known LV dysfunction (Zornoff et al., 2002) and right ventricular involvement during acute inferior myocardial infarction is a strong, independent predictor of major complications and in-hospital mortality (Zehender et al., 1993). Finally, 5–10% of patients with advanced chronic obstructive pulmonary disease (COPD) may suffer from severe pulmonary hypertension and present with a progressively downhill clinical course because of right heart failure added to the ventilatory handicap (Naeije, 2005).

In this context there is a need for a well-established animal model of right-sided HF for further investigation of RV function and pathology. Few animal models exist that are able to induce HF (whereas several models have been employed to induce RV hypertrophy, including monocrotaline (MCT) treatment (Jones et al., 2002; Jones et al., 2004; Kato et al., 2003), hypoxia (Bonnet et al., 2004; Pozeg et al., 2003), infarction (Nahrendorf et al., 2003) and also mild pulmonary trunk banding (PTB) (Adachi et al., 1995; Bar et al., 2003; Braun et al., 2003; Ikeda et al., 1999; Kuroha et al., 1991; Olivetti et al., 1988; Zierhut et al., 1990)). MCT treatment has been used to induce pulmonary hypertension resulting in RV hypertrophy and eventually HF (Chen et al., 2001; Doggrell and Brown, 1998). However, there are disadvantages to MCT in the form of disease manifestations not usually associated with human heart failure (hepatic cirrhosis and megalocytosis, venoocclusive disease and thrombocytopenia (Doggrell and Brown, 1998), and changes in hormones such as endothelin (Miyauchi et al., 1993)). PTB does not have the side-effects of MCT treatment and is a promising method for inducing symptomatic right-sided HF. Until now, the PTB HF model has not been characterized. The objective of this study was therefore to establish a rat model of right-sided heart failure using PTB and subsequently to characterize the systemic and cardiac changes in this model.

Upregulation of LV α-sarcomeric actin has been shown in rats with left-sided HF, possibly as a compensatory mechanism (Stilli et al., 2006). It has also been speculated that reductions in the level of sarcoplasmatic reticulum proteins involved in Ca^{2+} transport contribute to the pathophysiology of left-sided HF in humans (Movsesian et al., 1994). Using the PTB model, this study aimed to examine RV protein levels of α-sarcomeric actin and the calcium transporter SERCA2 in rats with right-sided HF.

Methods

Animals

Experiments were performed using male Wistar rats with an initial weight of 150–200 g. The rats were given free access to tap water and standard rat chow (Altromin #1324, Altromin, Lage, Germany) and were housed under controlled temperature ($21 \pm 2\,^{\circ}C$) and humidity ($55 \pm 2\%$) in a 12 h light-dark cycle. The animal protocols were approved by the boards of the Institute of Anatomy and Institute of Clinical Medicine, University of Aarhus, according to the licences for the use of experimental animals issued by the Danish Ministry of Justice.

Pulmonary trunk banding procedure

Rats were anesthetized with isoflurane (Forene–isoflurane, Abbot Scandinavia AB, Solona, Sweden) using an induction dose of 4% isoflurane in a mixture of 50% O_2 and 50% N_2O. In order to maintain sufficient ventilation throughout the procedure rats were intubated using a white venflon cut to a length of 4.1 cm and artificially ventilated using a rodent ventilator with a tidal volume of 3 ml and a rate of 75 breaths/min using 2% isoflurane in a mixture of 50% O_2, and 50% N_2O. In order to monitor cardiac status during surgery three electrodes, connected to a channel recorder (Power Lab 8 SP, channel recorder ML 785 SP, PowerLab-system, ADInstruments), were placed subcutaneously. Using a PC with PowerLab, Chart 5 software (ADInstruments) the signal from the channel recorder was translated into an ECG signal and displayed on a monitor. To minimize heat loss, all rats were placed on a heating pad during the whole procedure.

The chest was shaved and washed with alcohol before a 3 cm midline incision was made in the skin to reveal the pectoral muscles. Through an incision close to the sternum the left pectoral muscles were gently drawn aside thereby exposing the costae and intercostal muscles. The second, third, and sometimes fourth costae were cut with a pair of scissors. A retractor was inserted and used to push the costae away from the sternum making the thymus and heart accessible. The thymus was grasped with a clamped forceps and swung upwards. The pericardium was opened and using a dual view surgical microscope the pulmonary trunk was carefully separated from the aorta. Pulmonary trunk banding was done using titanium clips (Horizon

Ligating Clips ref. 001200, Weck Closure Systems). Often a 4.0 silk ligature was placed around the pulmonary trunk in order to ease placement of the clips. A modified Horizon applier (Horizon Applier, small, cat. nr. HZ137081, Weck Closure Systems, USA) was used to place and compress the clips around the pulmonary trunk. Before use the applier was adjusted to compress the clips to an outer diameter of 0.9 mm. When banding was successfully accomplished, the thymus was swung back and the retractor removed. Costae and intercostal muscles, the pectoral muscles and the skin were closed in three separate layers with Polysorb 4.0 suture. A small plastic tube connected to a 5 ml plastic syringe was left inside the thoracic cavity for drainage. Approximately 3 ml of air was evacuated from the thoracic cavity and while maintaining a negative pressure the tube was carefully retracted. This was done in order to re-establish the negative pressure necessary to unfold the lungs and minimize the risk of pneumothorax following the operation. All rats received a 4 ml isotonic saline injection subcutaneously to compensate for fluid loss during the procedure (bleeding and evaporation). When the animal showed sufficient spontaneous respiration and responded to handling, it was extubated. Prior to extubation the artificial ventilation was usually changed to 100% O_2. Rats were placed for up to 1 h inside a chamber with high oxygen concentration to help them recover before they were returned to their normal cage. To relieve postoperative pain, rats were treated with buprenorphine 0.12 mg/kg s.c. (Anorfin, GEA, Frederiksberg, Denmark) two times a day for 3 days. The first dose was always given at the start of the procedure. Sham operated animals underwent the same procedure as PTB rats except for banding of the pulmonary trunk.

Sacrificing procedures

In order to obtain information on the development and progression of PTB-induced HF, rats were operated and killed at different time points after PTB. Sham operation was performed in parallel and the Sham rats were paired with the PTB rats. Three groups were included in this study. Rats were killed 2–3, 5–7 or 16–17 weeks after banding, respectively. Six PTB and six Sham rats were selected for echocardiography 15 weeks after operation. All rats were maintained in metabolic cages 5 days prior to termination to allow urine collections for measuring Na^+, K^+, creatinine and osmolality. Subsequently the rats were anesthetized and right heart catheterization was performed (described below). Immediately after catheterization, a laparotomy was made and the peritoneum was inspected for ascites. If present, the amount was quantified by soaking up the fluid with a pre-weighed piece of soft paper and then weighing it again. Blood was collected from the aorta in a heparinized tube for subsequent analysis (described below). The liver was then removed, weighed and inspected for macroscopic signs of congestion (“nutmeg liver”). The thorax was opened and inspected for hydrothorax. If present, the fluid was collected and weighed. The heart was removed. Blood vessels and the heart atria were removed and the remainder of the heart was carefully washed and dissected into the RV and the LV with the septum attached (LV + S). The ventricles were then wiped clean from

fluids and blood and weighed. The following parameters were calculated: RV/body weight and LV + S/body weight.

Heart catheterization

Pressure measurements were done with a 1.4 Fr ultraminiature catheter pressure transducer (1.4 Fr SPR 671 Millar Instruments, Houston, TX) and a Pressure Control Unit (PCU-2000, Millar Instruments, Houston, TX) connected through a channel recorder (Power Lab 8 SP, channel recorder ML 785 SP, PowerLab-system, ADInstruments) to a PC with PowerLab, Chart 5 software (ADInstruments). An ECG was achieved via three electrodes placed subcutaneously on the rat. By modulating all input data the Chart 5 software made it possible to do simultaneous and continuous monitoring of ECG, blood pressure and rate of ventricular pressure rise and decay (dP/dT max and dP/dT min). Before each use the pressure was adjusted to zero by placing the catheter in a heparinized isotonic saline solution. The first zero calibration was done when the catheter had been placed in this solution for at least 30 min.

The animals were anesthetized with 2% isoflurane in a mixture of 50% O_2 and 50% N_2O, and placed on their back on a heating pad. Isoflurane was administered through a mask made for rodents and the rats maintained spontaneous breathing throughout the entire procedure. The right side of the neck was shaved and washed with alcohol. Using a pair of scissors a 3–4 cm incision was made in the skin in a direction from a little below the right clavicle towards the head. Under a dual view surgical microscope two forceps were used to free dissect the right jugular vein. A 4.0 silk ligature was placed around the proximal end of the vein. The distal end of the vein was ligated with a 4.0 silk ligature and a clamped forceps was placed at the end of the ligature to gently pull the vessel in the cranial direction. A small incision was made in the vein to expose the lumen and the catheter was introduced and advanced towards the right atrium. The proximal ligature was tightened to minimize bleeding. Once inside the atrium the catheter was advanced until the tip of the catheter was placed inside the RV. This was achieved by closely watching the blood pressure curve and observing the characteristic change of the pressure curve. The catheter was kept inside the RV for a few minutes to assure a reliable period used for calculating right ventricular systolic pressure (RVSP), right ventricular end diastolic pressure (RVEDP), dP/dT max, dP/dT min and heart rate. All results were calculated as the mean of 40 consecutive values recorded with Chart 5. Before the catheter was returned to the heparinized saline solution it was cleaned gently with a cotton swap. Some drifting from the zero set point occurred (a different value than the initial zero set point was recorded after the catheter had been returned to the heparinized saline solution). Because of this we decided to use a correction factor to compensate for drifting. The correction factor was calculated as the mean of the start zero value and the pressure value recorded after use of the catheter. The correction factor was used to correct RVSP and RVEDP.

Plasma and urine measurements

The rats were placed in metabolic cages (Techniplast, Italy) for a period of 5 days to enable urine collection. The plasma concentrations of electrolytes, urea, creatinine, bilirubin, albumin, alanine-amino-transferase (ALAT), alkaline phosphatase (ALP) and urine concentrations of creatinine and urea were determined (Vitros 950, Johnson & Johnson, USA).

Urine concentrations of sodium and potassium were determined by standard flame photometry (FCM 6341, Eppendorf, Germany). The osmolality of urine and plasma was determined by freezing point depression (Advanced Osmometer, Model 39000, Advanced Instruments, USA and Osmomat 030-D, Gonotec, Germany). The collected urine and plasma samples from the last 24 h of the study were used to determine renal creatinine clearance, using the formula $C = U \times V/P$ where C is renal clearance, U is urine concentration, V is urine flow rate and P is plasma concentration. To determine glomerular filtration rate (GFR) we assumed that renal clearance of creatinine equalled the GFR. Plasma concentration of aldosterone was also determined (Coat-A-Count Aldosterone, Diagnostic Products Corporation, LA, USA).

Semi-quantitative immunoblotting

The free-dissected RVs were homogenized in ice-cold isolation solution containing 0.3 M sucrose, 25 mM imidazole, 1 mM EDTA, 8.5 μM leupeptin and 1 mM phenylmethylsulfonyl fluoride, pH 7.2. The homogenates were centrifuged at 4000 rounds per minute for 15 min at 4 °C to remove whole cells, nuclei and mitochondria and the supernatant was pipetted off and kept on ice. All samples were solubilized at 90 °C for 10 min in Laemmli sample buffer, and then stored at −20 °C. To confirm equal loading an initial gel was stained with Coomassie Blue dye. SDS-PAGE was performed on 9% or 12% polyacrylamide gels. The proteins were transferred from the gel electrophoretically (BioRad Mini Protean II) to nitrocellulose membranes (Hybond ECL RPN3032D, Amersham Pharmacia Biotech, Little Chalfont, UK). After transfer the blots were blocked with 5% milk in PBS-T (80 mM Na2HPO4, 20 mM NaH_2PO_4, 100 mM NaCl, 0.1% Tween 20, pH 7.5) for 1 h and incubated overnight at 4 °C with primary antibodies. The sites of antibody-antigen reaction were visualized with horseradish peroxidase (HRP)-conjugated secondary antibodies (P447 or P448, diluted 1:3000; DAKO, Glostrup, Denmark) with an enhanced chemiluminescence system (ECL, Amersham Pharmacia Biotech, Little Chalfont, UK). The band densities were quantitated by scanning the densitometry and values were normalized to facilitate comparisons. Results are listed as the relative, not absolute, abundances between the groups, hence the term semiquantitative immunoblotting. The following commercial antibodies were used: mouse monoclonal anti-α-sarcomeric actin dilution 1:1000 and mouse monoclonal anti-SERCA2 ATPase dilution 1:1000, both from sigma-aldrich.

Histological examination

A 2-3 mm slice of the RV was cut. The tissue was immersion fixed by placing it in 4% paraformaldehyde buffer (pH 7) for at least 24 h. The tissue was dehydrated in graded ethanol and left overnight in xylene. After tissue embedding in paraffin 2 μm sections were cut on a rotary microtome (Leica Microsystems A/S, Herlev, Denmark). The sections were stained using collagen-specific Sirius Red to visualize fibrosis.

Echocardiography

Transthoracic echocardiography was performed in the supine or left lateral position, using inhalative anesthesia initially 4% then 1–2% isofluran, enriched with 1 l/min oxygen.

We used a Vivid 7 echocardiographic imaging unit (GE Medical Systems) equipped with a 10S 4–12 MHz transducer. The heart was imaged at a frame rate between 100 and 150 Hz and normally a second harmonic setting of 5.0/9.5 MHz was used. Two-dimensional (2D) echocardiographic images of a short-axis view on the mid-papillary level were recorded with the roundness of the left ventricular cavity as a criterion that the image was on axis. Great effort was taken to achieve a good image quality within the mid-papillary level to visualize the endo- and epicardial borders of the heart by carefully angulating and moving the transducer. Left and right ventricular areas were planimetered from the 2D recordings. Ejection fraction (EF) was calculated from these areas.

Statistical analyses

Values are presented as means ± standard errors (SE). The statistical significance of differences between the groups was determined using *F*-test test to determine variance and then using two-sample *t*-test. Multiple comparisons between the groups were analyzed by one-way analysis (ANOVA) followed by LSD for post hoc multiple comparisons test. P values <0.05 were considered significant.

Results

RV pressure measurements

RVSP, RVEDP, dP/dT max and dP/dT min values are plotted in Fig. 1. PTB rats had markedly increased RVSP from the beginning and throughout the study. At 2–3 weeks after banding PTB rat RVSP was tripled compared to Sham rats (87.8 ± 6.8 vs. 28.1 ± 1.7 mmHg in Sham rats, $p<0.05$). PTB rat RVSP reached a maximum at 5–7 weeks after banding (114.3 ± 7.1 vs. 36.1 ± 1.7 mmHg in Sham rats, $p<0.05$) and stabilized around the maximum value during the rest of the study period. Sham rat

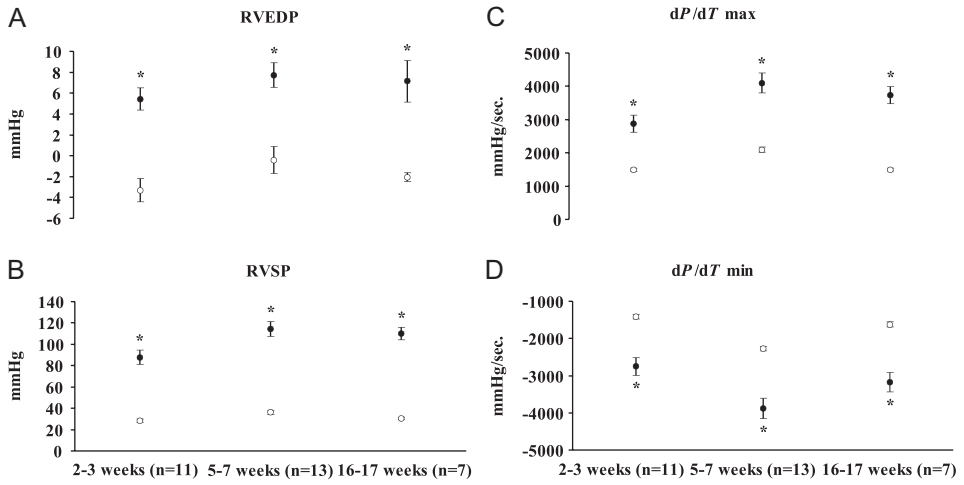

Fig. 1. Hemodynamic parameters in PTB-induced pressure overload. Values are plotted as means $\pm$ SE. *$p < 0.05$. Black circles indicate PTB values and white circles indicate Sham values. (A) RVEDP, right ventricular end diastolic pressure, (B) RVSP, right ventricular systolic pressure, (C) dP/dT max, rate of pressure rise, and (D) dP/dT min, rate of pressure decay. The numbers of PTB rats in each group are given in parentheses. An equal number of Sham animals were included in each group. Note the markedly increased pressures in the PTB rats from the beginning of the study.

RVSP values were stable throughout the study. Preload in PTB rats was markedly increased evidenced by a significantly increased RVEDP throughout the study. At 2–3 weeks after banding, PTB rat RVEDP was almost tripled compared to Sham rats (5.4 ± 1.1 vs. -3.3 ± 1.1 mmHg in Sham rats, $p < 0.05$) and stabilized at this level during the rest of the study period. dP/dT max was also significantly increased in PTB rats in all groups. At 2–3 weeks after banding dP/dT max was doubled compared to Sham rats (2880 ± 255 vs. 1486 ± 56 mmHg/s in Sham rats, $p < 0.05$) and reached a maximum at 5–7 weeks after banding (4101 ± 303 vs. 2093 ± 75 mmHg/s in Sham rats, $p < 0.05$) where it stabilized for the rest of the study period. The increase in dP/dT max can be ascribed to the increased preload but may also suggest an increased myocardial contractility.

Ventricular hypertrophy

PTB produced pronounced RV hypertrophy from the beginning and throughout the study (Figs. 2 and 3). Marked fibrosis was present 3 weeks after PTB (Fig. 3). Compared with Sham rats, 2–3 weeks after banding of the pulmonary trunk, RV weight in PTB rats was doubled (0.38 ± 0.02 vs. 0.19 ± 0.01 g in Sham rats, $p < 0.05$). Maximal RV hypertrophy was observed 16–17 weeks after banding (0.55 ± 0.03 vs. 0.19 ± 0.01 g in Sham rats, $p < 0.05$) which was significantly higher than the other PTB groups, showing that RV hypertrophy is indeed a long-term process in the PTB

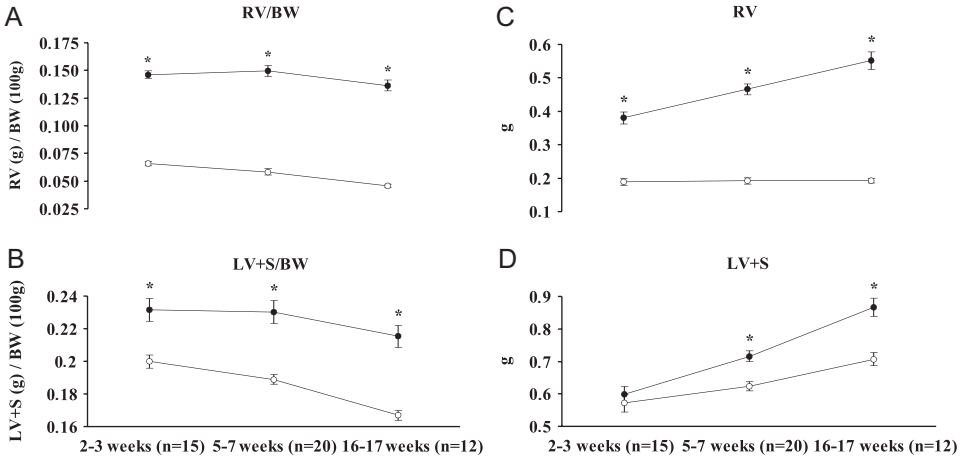

Fig. 2. Cardiac hypertrophy in PTB induced pressure overload. Values are plotted as means ± SE. *$p < 0.05$. Black circles indicate PTB values and white circles indicate Sham values. Weight of the right ventricle (RV) and left ventricle (LV) ($C + D$) is shown along with the weights adjusted for body weight (BW) ($A + B$). The numbers of PTB rats in each group are given in parentheses. An equal number of Sham animals were included in each group. Note the excessive RV hypertrophy in PTB rats and the less pronounced hypertrophy of the LV.

model. When adjusted for body weight, the increase in RV weight was partially masked by a corresponding increase in body weight but there was a significant difference between PTB and Sham rats in all groups. When adjusted for body weight, significant hypertrophy of the LV + S was present in all groups, although this hypertrophy was much less pronounced than the hypertrophy of the RV. Looking at the unadjusted weights, maximal LV hypertrophy was observed 16–17 weeks after banding (0.87 ± 0.03 vs. 0.71 ± 0.02 g in Sham rats, $p < 0.05$) which was significantly higher than the other PTB groups.

Plasma and urine analyses

Plasma values and creatinine clearance are plotted in Table 1. Plasma potassium was increased in the 2–3 weeks PTB group compared with Sham rats (5.97 ± 0.27 vs. 5.06 ± 0.1 mmol/l in Sham rats, $p < 0.05$) but no significant differences were seen in the other groups. Significant elevation of plasma urea was seen in all PTB groups compared with Sham rats. GFR estimated as creatinine clearance was significantly reduced in the 2–3 weeks PTB group (4.2 ± 0.3 vs. 5.3 ± 0.3 ml/min/kg in Sham rats, $p < 0.05$) and 16–17 weeks PTB group (3.6 ± 0.2 vs. 5.2 ± 0.2 ml/min/kg in Sham rats, $p < 0.05$) but not in the 5–7 weeks group. The decrease in GFR taken together with increased plasma urea levels and the hyperkaleamia observed in the 2–3 weeks PTB group indicated renal failure. Plasma alkaline phosphatase (ALP) was significantly increased in all PTB groups. PTB rats had significantly higher plasma aldosterone

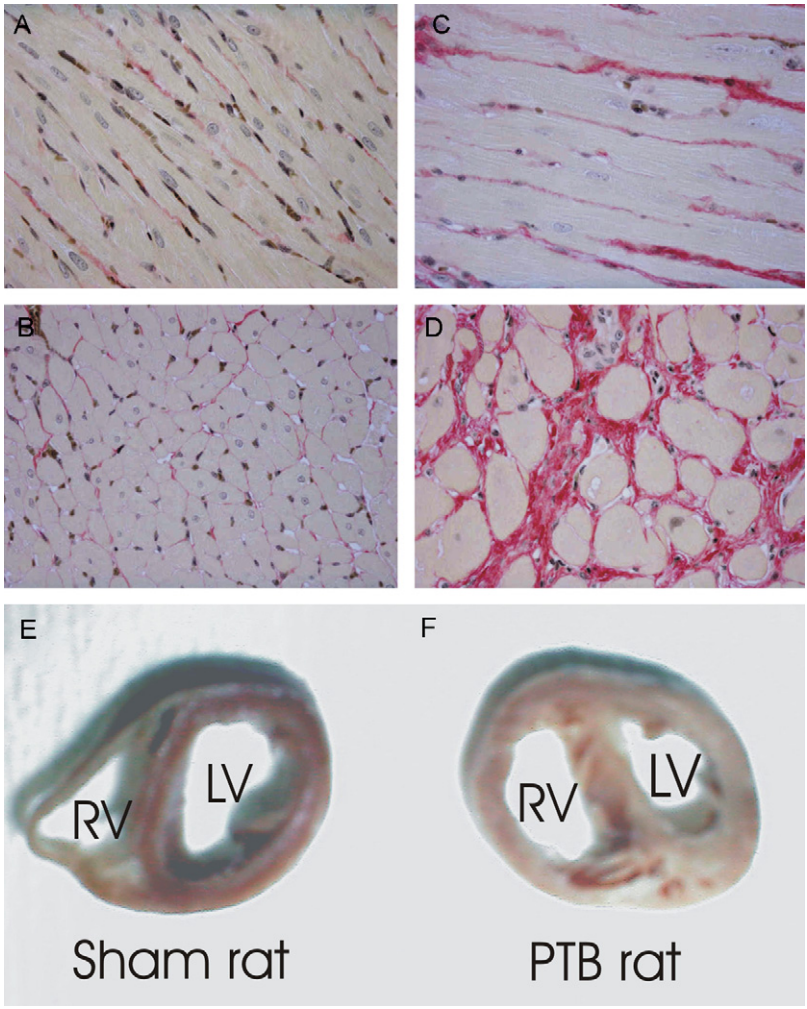

Fig. 3. Cardiac fibrosis and hypertrophy in PTB induced pressure overload. Sections from Sham animals ($A+B$) and sections from PTB animals ($C+D$) are shown. All sections are at the same magnification. Note the increased cardiomyocyte size and the increased fibrosis in PTB animals. Note the macroscopic hypertrophy of the right ventricle (RV) in the PTB rat (F) compared to the Sham rat (E).

levels in the 2–3 weeks group (771 ± 113 vs. 402 ± 33 pg/ml, $p < 0.05$) but no changes were observed in the other groups (data not shown).

Signs of backward failure

Ascites, hydrothorax and congestion of the liver were prominent findings in PTB rats in all groups although only some rats in each group were affected. When present,

Table 1. Changes in liver and renal function

	2–3 weeks		5–7 weeks		16–17 weeks	
	Sham (14)	PTB (21)	Sham (20)	PTB (16)	Sham (8)	PTB (7)
P_K (mmol/l)	5.1±0.1	6.0±0.3*	5.3±0.2	5.5±0.1	5.1±0.6	5.3±0.3
P_{crea} (μmol/l)	29,4±1.7	38.0±3.3*	48.2±2.7	49.2±2.3	39.4±0.9	54.0±5.5*
P_{urea} (mmol/l)	5.9±0.1	7.0±0.2*	6.7±0.2	8.3±0.3*	7.3±0.3	8.9±0.6*
P_{ALP} (U/l)	219±9	294±11*	137±5	188±12*	105±7	160±7*
C_{cr} (ml/min/kg)	5.3±0.3	4.2±0.3*	3.6±0.2	3.4±0.1	5.2±0.2	3.6±0.2*

Values are expressed as means±SE. Numbers in parentheses give the number of rats that were used for plasma analyses. P_K, plasma potassium; P_{crea}, plasma creatinine; P_{urea}, plasma urea; P_{ALP}, plasma alkaline phosphatase; C_{cr}, creatinine clearance.

*$p<0.05$.

Table 2. Signs of backward failure

Total number of rats	2–3 weeks		5–7 weeks		16–17 weeks	
	Sham (20)	PTB (29)	Sham (16)	PTB (21)	Sham (14)	PTB (14)
Body weight (g)	268±10	245±8	330±5	313±6*	424±10	403±8
Ascites	—	24%	—	14%	—	29%
Hydrothorax	—	34%	—	24%	—	43%
Liver congestion	—	31%	—	29%	—	43%

Values are expressed as means±SE or as percentages. The prevalence of ascites, hydrothorax and liver congestion among rats is expressed as percentages of the total number of rats. No Sham rats had any detectable amounts of effusions. When present, the amount of ascites was between 1 and 4 g and the amount of hydrothorax was between 0.25 and 23 g.

*$p<0.05$.

the amount of ascites was between 1 and 4 g and the amount of hydrothorax was between 0.25 and 23 g, showing the broad spectrum of disease manifestation. The percentages of PTB rats in each group with hydrothorax, ascites or macroscopic signs of congestion of the liver are shown in Table 2. Congestion of the liver and presence of hydrothorax was most prominent in the 16–17 weeks group with a prevalence of 43% among the PTB rats. The prevalence of ascites was also greatest in the 16–17 weeks group. No Sham rats showed ascites, hydrothorax or congestion of the liver.

Echocardiography

To evaluate RV and LV function, echocardiography was performed on six PTB and six Sham rats 15 weeks after PTB-operation (Fig. 4). PTB rat LV diastolic lumen was decreased compared to Sham rats (0.27±0.07 vs. 0.44±0.06 cm^2, $p<0.05$). Conversely, RV diastolic lumen was increased compared to Sham rats (0.43±0.12 vs. 0.13±0.03 cm^2, $p<0.05$). LV systolic lumen was unchanged compared to Sham

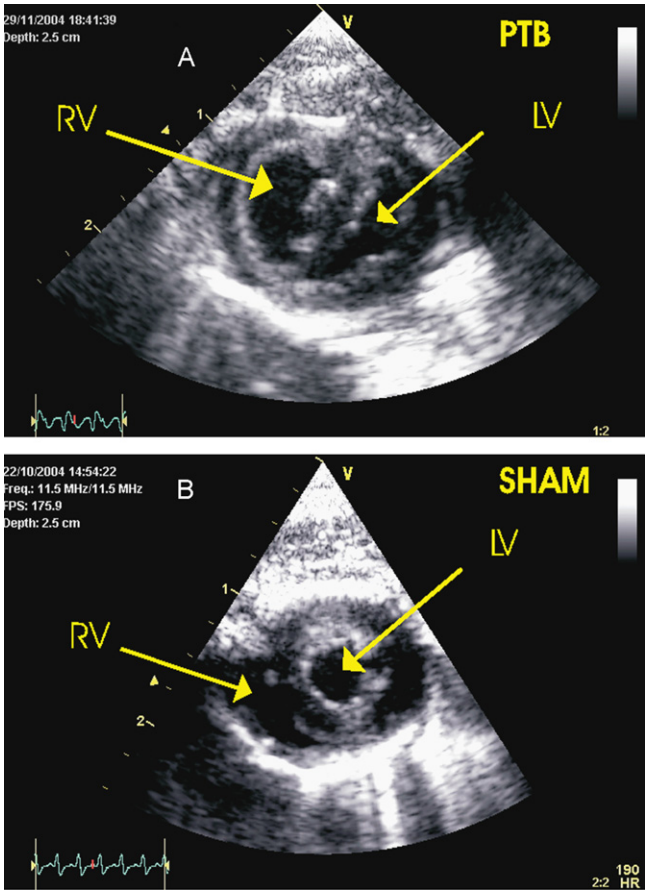

Fig. 4. Two-dimensional (2D) echocardiographic images 15 weeks after PTB (A) or Sham (B) operation. Short-axis view on the mid-papillary level. Note the pronounced hypertrophy and dilation of the PTB rat RV compared to Sham rat RV. Also note the deviation of the interventricular septum into the LV.

rats. RV systolic lumen was increased compared to Sham rats (0.30 ± 0.14 vs. $0.05 \pm 0.01\,cm^2$, $p < 0.05$). LV EF was unchanged compared to Sham rats (64.5 ± 18.8 vs. $69.4 \pm 6.36\%$, $p = 0.56$). RV EF was decreased compared to Sham rats (33.5 ± 16.0 vs. $65.8 \pm 9.75\%$, $p < 0.05$). The fact that LV diastolic lumen was decreased and that LV EF was unchanged strongly indicated that PTB rats had reduced cardiac output.

Immunoblotting

RV protein levels of SERCA2 and α-sarcomeric actin were determined in seven PTB rats and six Sham rats from the 2–3 weeks group. To identify SERCA2 and

α-sarcomeric actin, specific monoclonal antibodies were used (as described in the Methods section). There was no significant difference between PTB rat RV myocardium and Sham rat RV myocardium for either SERCA2 or α-sarcomeric actin (Figs. 5 and 6).

Discussion

Defining HF in an animal model

Defining HF is challenging since there are neither objective cut-off values of cardiac or ventricular dysfunction nor changes in flow, pressure, dimension or volume that can be reliably used to identify patients with HF (Swedberg et al., 2005). The European Society of Cardiology task force for the diagnosis and treatment of congestive HF states that both symptoms at rest or during exertion as well as objective evidence of cardiac dysfunction at rest must be present to diagnose HF (Swedberg et al., 2005). Obviously, in an animal model of HF symptoms such as fatigue or breathlessness are difficult to detect and quantify. Thus, very few studies have employed animal models of right-sided HF and often rather loose criteria for HF diagnosis (such as ruffled fur or weight loss combined with cardiac hypertrophy) have been used (LekanneDeprez et al., 1998). Studies of left-sided HF are much better established but still do not address symptoms. Hence, evaluation of the models rely on objective findings such as increased filling pressures, reduced cardiac output and reduced ejection fraction (Chen et al., 2001; Heyen et al., 2002; Pfeffer et al., 1979; Staahltoft et al., 2002). Additional valuable signs of backward failure are

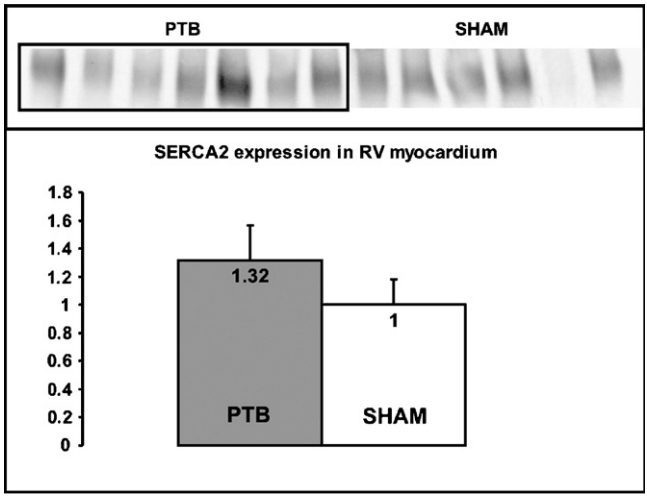

Fig. 5. Immunoblot showing specific bands corresponding to SERCA2 (top) and a bar graph (bottom) showing the relative difference between PTB and Sham rat SERCA2 protein levels.

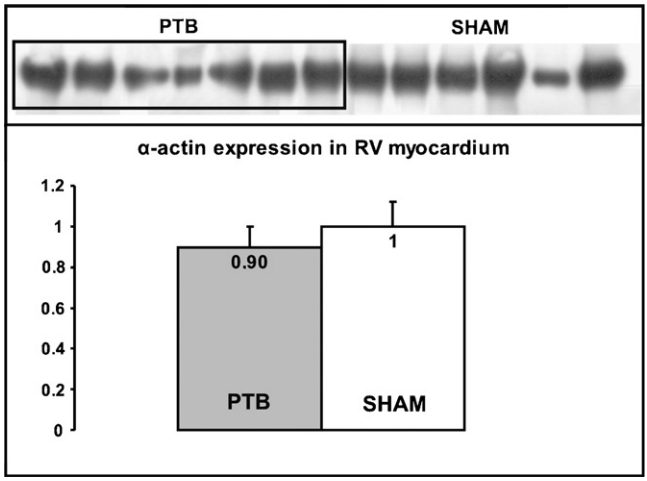

Fig. 6. Immunoblot showing specific bands corresponding to α-sarcomeric actin (top) and a bar graph (bottom) showing the relative difference between PTB and Sham rat α-sarcomeric actin protein levels.

ascites and hydrothorax (Shigematsu et al., 2001). Thus, in an animal model of HF the consensus is that objective findings of cardiac dysfunction are sufficient to define HF, especially if concomitant signs of backward failure are present.

Present findings vs. previous studies

The results of this study characterize PTB as a method for inducing right-sided HF in rats. This is based on the consistent and numerous pathologic objective findings in the different groups. In the present study PTB was associated with RVSP values up to 120 mmHg and a 200% increase in RV weight along with severe signs of backward failure in the form of ascites and hydrothorax formation as well as congestion of the liver accompanied by elevated liver enzymes. In addition, changes in renal function were found in some groups and echocardiography revealed reduced LV dimension and substantially decreased RV EF. In comparison, studies using MCT treatment have only achieved RVSP values between 40 and 77 mmHg and a 100–200% increase in RV weight and most studies do not report formation of ascites or hydrothorax (Chen et al., 2001; Jones et al., 2004; Kogler et al., 2003; Leineweber et al., 2002; Miyauchi et al., 1993; Seyfarth et al., 2000). Previous studies have mainly used PTB for hypertrophy research. These studies achieved RVSP values between 30 and 77 mmHg and a 50–100% increase in RV weight (Adachi et al., 1995; Ikeda et al., 1999; Olivetti et al., 1988; Zierhut et al., 1990; Zimmer, 1992). The differences between previous hypertrophy studies and the present HF study were probably due to a much higher degree of constriction of the pulmonary artery in our PTB model (0.9 mm vs. 1.7–1.1 mm in other studies). To the best of our knowledge only one previous study has used PTB to induce overt HF and it lacked information on

important parameters such as RV pressures since its focus was not on characterization of the PTB HF model (LekanneDeprez et al., 1998).

Immunoblotting for SERCA2 and α-sarcomeric actin revealed no significant changes. SERCA2 protein levels from failing LVs have been examined in several studies, most of which found no significant changes (Movsesian et al., 1994; Schwinger et al., 1995; Linck et al., 1996). This study showed that SERCA2 was not changed in failing RVs either. Thus, down-regulation of SERCA2 most likely does not play a role in either right or left-sided heart failure. Upregulation of LV α-sarcomeric actin has been shown in rats with left-sided HF, possibly as a compensatory mechanism (Stilli et al., 2006). This study could not show any upregulation of α-sarcomeric actin in failing RVs, although compensatory hypertrophy was present. Further studies are required to confirm this finding.

Time course

Development of HF in this model occurred early in the study as signs of backward failure were present 2–3 weeks after banding and development of HF probably occurred right after banding. This was in contrast to the MCT model in which pulmonary hypertension slowly progresses and leads to HF after a considerable number of weeks. There was no substantial progression of heart failure symptoms throughout the study period (the prevalence of ascites, hydrothorax and liver congestion remained largely the same in all the PTB groups) whereas the heart (RV and LV) continued to hypertrophy until the end of the study period. The lack of progression of heart failure could be explained by the hypertrophy observed, which partly compensated for banding of the pulmonary artery. Marked fibrosis was present from 3 weeks after PTB underscoring that remodelling takes place soon after banding.

Inter-individual variations

It was evident that animals within the groups reacted differently to the banding since only some of the PTB rats in each group showed signs of backward failure. PTB using surgical nylon thread has been used in several hypertrophy experiments. However, slippage of the band and the obvious difficulties ensuring the same degree of constriction among the banded animals when using a surgical nylon thread led us to believe that banding with titanium clips would be a more reliable method to create PTB HF rats. Indeed, in another PTB study using surgical nylon thread, about 25% of the banded rats showed no hypertrophy (LekanneDeprez et al., 1998) suggesting that this was a less reliable way of banding. As all PTB rats in this study showed pronounced hypertrophy, banding with clips was a very reliable method. Variation of disease manifestations is apparent in all animal HF studies and this PTB HF study was no exception. However, the prevalence of signs of backward failure in this study was generally higher than MCT studies underscoring the effectiveness of the PTB model.

Ventricular interdependence

The presence of ventricular interdependence was also evident as mild hypertrophy of the LV + S was observed in the groups. Whether this hypertrophy of the LV + S was actually due to septum hypertrophy alone or also due to hypertrophy of the LV is unknown, as we did not weigh the septum and the LV separately. However, recent results demonstrated that pulmonary hypertension was associated with a decrease in the size of LV whereas the septum hypertrophied (Boer et al., 2005). The presence of renal failure in some of the PTB groups in this study suggested that LV dysfunction was considerable, as a rather great decrease in cardiac output (causing pre-renal azotaemia) is necessary for changes in GFR to occur due to renal auto regulation. Echocardiography 15 weeks after PTB showed decreased LV diastolic dimension and unchanged LV EF indicating that PTB rats had reduced cardiac output.

In summary, a reproducible animal model of right-sided HF has been established using titanium clips to induce a mechanical overload of the RV. PTB selectively affects the heart and does not have the side-effects of MCT treatment which makes PTB a superior hypertrophy and HF model. The novelty of this PTB model compared to previous PTB models was that we were able to induce overt heart failure rather than just RV hypertrophy. Most HF studies focus on cardiac changes only. We have examined not only the haemodynamic and structural changes in the RV but also the pathophysiological changes in other organs including plasma and renal function changes which provides valuable additional information. The long time-course of our study enables PTB to be used for experiments in both acute/subacute (few weeks) and chronic (17 weeks) heart failure. The presence of three separate PTB groups at different time-points clearly illustrated the development of hypertrophy and RV pressures as well as the development of extra-cardiac manifestations. It is the hope and belief of the authors that this study will provide researchers with a reproducible and reliable method for experimentally inducing right-sided heart failure so that an important area of human heart disease may be explored further.

Acknowledgements

The authors thank Gitte Kall and Lotte Valentin for expert technical assistance. The Water and Salt Research Centre at the University of Aarhus is established and supported by the Danish National Research Foundation (Danmarks Grundforskningsfond). Support for this study was provided by The Karen Elise Jensen Foundation, The Commission of the European Union (QRLT-2000-00987 and QLRT-2000-00778), The Human Frontier Science Program, The WIRED program (Nordic Council and the Nordic Centre of Excellence Program in Molecular Medicine), The Novo Nordisk Foundation, The Danish Medical Research Council, The University of Aarhus Research Foundation, The University of Aarhus, The Hede Nielsen Foundation and The Helen, The Ejnar Bjørnow Foundation and The Grosserer L.F. Foghts Foundation.

References

Adachi, S., Ito, H., Ohta, Y., Tanaka, M., Ishiyama, S., Nagata, M., Toyozaki, T., Hirata, Y., Marumo, F., Hiroe, M., 1995. Distribution of mRNAs for natriuretic peptides in RV hypertrophy after pulmonary arterial banding. Am. J. Physiol. 268, H162–H169.

Bar, H., Kreuzer, J., Cojoc, A., Jahn, L., 2003. Upregulation of embryonic transcription factors in right ventricular hypertrophy. Basic Res. Cardiol. 98, 285–294.

Boer, C., Waard, M., Simonides, W.S., Duncker, D.J., 2005. Left ventricular remodeling after monocrotaline-induced pulmonary hypertension in mice. FASEB J. 19, 1332.

Bonnet, P.S., Bonnet, J., Boissiere, J.L., Le Net, M., Gautier, R.E., Dumas de la Roque, E., Eder, V., 2004. Chronic hypoxia induces nonreversible right ventricle dysfunction and dysplasia in rats. Am. J. Physiol. Heart Circ. Physiol. 287, H1023–H1028.

Braun, M.U., Szalai, P., Strasser, R.H., Borst, M.M., 2003. Right ventricular hypertrophy and apoptosis after pulmonary artery banding: regulation of PKC isozymes. Cardiovasc. Res. 59, 658–667.

Chen, L., Gan, X.T., Haist, J.V., Feng, Q., Lu, X., Chakrabarti, S., Karmazyn, M., 2001. Attenuation of compensatory right ventricular hypertrophy and heart failure following monocrotaline-induced pulmonary vascular injury by the Na+–H+ exchange inhibitor cariporide. J. Pharmacol. Exp. Ther. 298, 469–476.

Clyne, C.A., Alpert, J.S., Benotti, J.R., 1989. Interdependence of the left and right ventricles in health and disease. Am. Heart J. 117, 1366–1373.

Dittrich, H.C., Chow, L.C., Nicod, P.H., 1989. Early improvement in left ventricular diastolic function after relief of chronic right ventricular pressure overload. Circulation 80, 823–830.

Doggrell, S.A., Brown, L., 1998. Rat models of hypertension, cardiac hypertrophy and failure. Cardiovasc. Res. 39, 89–105.

Heyen, J.R., Blasi, E.R., Nikula, K., Rocha, R., Daust, H.A., Frierdich, G., Van Vleet, J.F., De, C.P., McMahon, E.G., Rudolph, A.E., 2002. Structural, functional, and molecular characterization of the SHHF model of heart failure. Am. J. Physiol Heart Circ. Physiol. 283, H1775–H1784.

Hill, M.F., Singal, P.K., 1997. Right and left myocardial antioxidant responses during heart failure subsequent to myocardial infarction. Circulation 96, 2414–2420.

Ikeda, S., Hamada, M., Hiwada, K., 1999. Cardiomyocyte apoptosis with enhanced expression of P53 and Bax in right ventricle after pulmonary arterial banding. Life Sci. 65, 925–933.

Jones, J., Mendes, E.L., Rudd, M.A., Russo, G., Loscalzo, J., Zhang, Y.Y., 2002. Serial noninvasive assessment of progressive pulmonary hypertension in a rat model. Am. J. Physiol. Heart Circ. Physiol. 283, H364–H371.

Jones, J.E., Walker, J.L., Song, Y., Weiss, N., Cardoso, W.V., Tuder, R.M., Loscalzo, J., Zhang, Y.Y., 2004. Effect of 5-lipoxygenase on the development of pulmonary hypertension in rats. Am. J. Physiol. Heart Circ. Physiol. 286, H1775–H1784.

Kato, Y., Iwase, M., Kanazawa, H., Kawata, N., Yoshimori, Y., Hashimoto, K., Yokoi, T., Noda, A., Takagi, K., Koike, Y., Nishizawa, T., Nishimura, M., Yokota, M., 2003. Progressive development of pulmonary hypertension leading to right ventricular hypertrophy assessed by echocardiography in rats. Exp. Anim. 52, 285–294.

Kogler, H., Hartmann, O., Leineweber, K., Nguyen, v.P., Schott, P., Brodde, O.E., Hasenfuss, G., 2003. Mechanical load-dependent regulation of gene expression in monocrotaline-induced right ventricular hypertrophy in the rat. Circ. Res. 93, 230–237.

Kuroha, M., Isoyama, S., Ito, N., Takishima, T., 1991. Effects of age on right ventricular hypertrophic response to pressure-overload in rats. J. Mol. Cell. Cardiol. 23, 1177–1190.

Leineweber, K., Brandt, K., Wludyka, B., Beilfuss, A., Ponicke, K., Heinroth-Hoffmann, I., Brodde, O.E., 2002. Ventricular hypertrophy plus neurohumoral activation is necessary to alter the cardiac beta-adrenoceptor system in experimental heart failure. Circ. Res. 91, 1056–1062.

LekanneDeprez, R.H., van den Hoff, M.J., de Boer, P.A., Ruijter, P.M., Maas, A.A., Chamuleau, R.A., Lamers, W.H., Moorman, A.F., 1998. Changing patterns of gene expression in the pulmonary trunk-banded rat heart. J. Mol. Cell. Cardiol. 30, 1877–1888.

Linck, B., Boknik, P., Eschenhagen, T., Muller, F.U., Neumann, J., Nose, M., Jones, L.R., Schmitz, W., Scholz, H., 1996. Messenger RNA expression and immunological quantification of Phospholamban and SR-Ca(2+)-ATPase in failing and nonfailing human hearts. Cardiovasc. Res. 31, 625–632.

Miyauchi, T., Yorikane, R., Sakai, S., Sakurai, T., Okada, M., Nishikibe, M., Yano, M., Yamaguchi, I., Sugishita, Y., Goto, K., 1993. Contribution of endogenous endothelin-1 to the progression of cardiopulmonary alterations in rats with monocrotaline-induced pulmonary hypertension. Circ. Res. 73, 887–897.

Mizushige, K., Morita, H., Senda, S., Matsuo, H., 1989. Influence of right ventricular pressure overload on left and right ventricular filling in cor pulmonale assessed with Doppler echocardiography. Jpn Circ. J. 53, 1287–1296.

Movsesian, M.A., Karimi, M., Green, K., Jones, L.R., 1994. Ca(2+)-transporting ATPase, phospholamban, and calsequestrin levels in nonfailing and failing human myocardium. Circulation 90, 653–657.

Naeije, R., 2005. Pulmonary hypertension and right heart failure in chronic obstructive pulmonary disease. Proc. Am. Thorac. Soc. 2, 20–22.

Nahrendorf, M., Hu, K., Fraccarollo, D., Hiller, K.H., Haase, A., Bauer, W.R., Ertl, G., 2003. Time course of right ventricular remodeling in rats with experimental myocardial infarction. Am. J. Physiol. Heart Circ. Physiol. 284, H241–H248.

Olivetti, G., Ricci, R., Lagrasta, C., Maniga, E., Sonnenblick, E.H., Anversa, P., 1988. Cellular basis of wall remodeling in long-term pressure overload-induced right ventricular hypertrophy in rats. Circ. Res. 63, 648–657.

Pfeffer, M.A., Pfeffer, J.M., Fishbein, M.C., Fletcher, P.J., Spadaro, J., Kloner, R.A., Braunwald, E., 1979. Myocardial infarct size and ventricular function in rats. Circ. Res. 44, 503–512.

Pozeg, Z.I., Michelakis, E.D., McMurtry, M.S., Thebaud, B., Wu, X.C., Dyck, J.R., Hashimoto, K., Wang, S., Moudgil, R., Harry, G., Sultanian, R., Koshal, A., Archer, S.L., 2003. In vivo gene transfer of the O2-sensitive potassium channel Kv1.5 reduces pulmonary hypertension and restores hypoxic pulmonary vasoconstriction in chronically hypoxic rats. Circulation 107, 2037–2044.

Schwinger, R.H., Bohm, M., Schmidt, U., Karczewski, P., Bavendiek, U., Flesch, M., Krause, E.G., Erdmann, E., 1995. Unchanged protein levels of SERCA II and phospholamban but reduced Ca2+ uptake and Ca(2+)-ATPase activity of cardiac sarcoplasmic reticulum from dilated cardiomyopathy patients compared with patients with nonfailing hearts. Circulation 92, 3220–3228.

Seyfarth, T., Gerbershagen, H.P., Giessler, C., Leineweber, K., Heinroth-Hoffmann, I., Ponicke, K., Brodde, O.E., 2000. The cardiac beta-adrenoceptor-G-protein(s)-adenylyl cyclase system in monocrotaline-treated rats. J. Mol. Cell. Cardiol. 32, 2315–2326.

Shigematsu, H., Hirooka, Y., Eshima, K., Shihara, M., Tagawa, T., Takeshita, A., 2001. Endogenous angiotensin II in the NTS contributes to sympathetic activation in rats with aortocaval shunt. Am. J. Physiol. Regul. Integr. Comp. Physiol. 280, R1665–R1673.

Staahltoft, D., Nielsen, S., Janjua, N.R., Christensen, S., Skott, O., Marcussen, N., Jonassen, T.E., 2002. Losartan treatment normalizes renal sodium and water handling in rats with mild congestive heart failure. Am. J. Physiol. Renal Physiol. 282, F307–F315.

Stilli, D., Bocchi, L., Berni, R., Zaniboni, M., Cacciani, F., Chaponnier, C., Musso, E., Gabbiani, G., Clement, S., 2006. Correlation of alpha-skeletal actin expression, ventricular fibrosis and heart function with the degree of pressure overload cardiac hypertrophy in rats. Exp. Physiol. 91, 571–580.

Swedberg, K., Cleland, J., Dargie, H., Drexler, H., Follath, F., Komajda, M., Tavazzi, L., Smiseth, O.A., Gavazzi, A., Haverich, A., Hoes, A., Jaarsma, T., Korewicki, J., Levy, S., Linde, C., Lopez-Sendon, J.L., Nieminen, M.S., Pierard, L., Remme, W.J., 2005. Guidelines for the diagnosis and treatment of chronic heart failure: executive summary (update 2005): The Task Force for the Diagnosis and Treatment of Chronic Heart Failure of the European Society of Cardiology. Eur. Heart J. 26, 1115–1140.

Yu, C.M., Sanderson, J.E., Chan, S., Yeung, L., Hung, Y.T., Woo, K.S., 1996. Right ventricular diastolic dysfunction in heart failure. Circulation 93, 1509–1514.

Zehender, M., Kasper, W., Kauder, E., Schonthaler, M., Geibel, A., Olschewski, M., Just, H., 1993. Right ventricular infarction as an independent predictor of prognosis after acute inferior myocardial infarction. N. Engl. J. Med. 328, 981–988.

Zierhut, W., Zimmer, H.G., Gerdes, A.M., 1990. Influence of ramipril on right ventricular hypertrophy induced by pulmonary artery stenosis in rats. J. Cardiovasc. Pharmacol. 16, 480–486.

Zimmer, H.G., 1992. Development and modulation of experimental right ventricular hypertrophy in rats. J. Cardiovasc. Pharmacol. 20 (Suppl 1), S1–S6.

Zornoff, L.A., Skali, H., Pfeffer, M.A., St John, S.M., Rouleau, J.L., Lamas, G.A., Plappert, T., Rouleau, J.R., Moye, L.A., Lewis, S.J., Braunwald, E., Solomon, S.D., 2002. Right ventricular dysfunction and risk of heart failure and mortality after myocardial infarction. J. Am. Coll. Cardiol. 39, 1450–1455.